SSC18-V-05

CubeX: A compact X-Ray Telescope Enables both X-Ray Fluorescence Imaging Spectroscopy and Pulsar Timing Based Navigation

Jan Stupl, Monica Ebert, David Mauro
SGT / NASA Ames
NASA Ames Research Center, Moffett Field, CA; 650-604-4032
jan.stupl@nasa.gov

JaeSub Hong
Harvard University
Cambridge, MA

Suzanne Romaine, Almus Kenter, Janet Evans, Ralph Kraft
Smithsonian Astrophysical Observatory
Cambridge, MA

Larry Nittler
Carnegie Institution of Washington
Washington, DC

Ian Crawford
Birkbeck College
London, UK

David Kring
Lunar and Planetary Institute
Houston, TX

Noah Petro, Keith. Gendreau, Jason Mitchell, Luke Winternitz
NASA Goddard Space Flight Center
Greenbelt, MD

Rebecca. Masterson, Gregory Prigozhin
Massachusetts Institute of Technology
Cambridge, MA

Brittany Wickizer
NASA Ames Research Center
Moffett Field, CA

Kellen Bonner, Ashley Clark, Arwen Dave, Andres Dono-Perez, Ali Kashani, Daniel Larrabee, Samuel Montez, Karolyn Ronzano, Tim Snyder
MEI / NASA Ames Research Center

Joel Mueting, Laura Plice
Metis / NASA Ames Research Center
NASA Ames Research Center, Moffett Field, CA

Yueh-Liang Shen, Duy Nguyen
Booz Allen Hamilton / NASA Ames
NASA Ames Research Center, Moffett Field, CA

ABSTRACT

This paper describes the miniaturized X-ray telescope payload, *CubeX*, in the context of a lunar mission. The first part describes the payload in detail, the second part summarizes a small satellite mission concept that utilizes its compact form factor and performance. This instrument can be used for both X-ray fluorescence (XRF) imaging spectroscopy and X-ray pulsar timing-based navigation (XNAV). It combines high angular resolution (<1 arcminutes) Miniature Wolter-I X-ray optics (MiXO) with a common focal plane consisting of high spectral resolution (<150 eV at 1 keV) CMOS X-ray sensors and a high timing resolution (< 1 μsec) SDD X-ray sensor. This novel combination of the instruments enables both XRF measurements and XNAV operations without moving parts, in a small form factor (~1×1×6U, <6 kg). In this paper we illustrate one potential application for a lunar mission concept: The elemental composition of the Moon holds keys to understanding the origin and evolution of both the Moon and the Earth. X-ray fluorescence (XRF), induced either by solar X-ray flux or energetic ions, carries decisive signatures of surface elemental composition. In between XRF observations, *CubeX* also leverages the technology of high resolution X-ray imaging and time series measurements to conduct XNAV operations and evaluate their performance.

INTRODUCTION

This paper introduces a novel X-ray imaging spectrometer (XIS) payload, the *CubeX* instrument. The instrument can be used both for X-ray fluorescence measurements and X-ray pulsar timing measurements for absolute navigation.

Remote sensing XRF measurements provide insight into the geology of planetary bodies. While laboratory analysis of returned samples and in situ (e.g., rover and human) analyses provide the most detailed and accurate abundance measurements of individual rocks, remote sensing from orbiting spacecraft (S/C) remains the best method for larger-scale geochemical measurements of planetary bodies. Methods used for elemental remote sensing of rocky bodies include X-ray, gamma-ray, neutron, and reflectance spectroscopy. Only the first two provide the direct measurement of specific rock-forming elements and are, thus, of great importance to mapping planetary compositions. Remote-sensing X-ray fluorescence (XRF) spectroscopy allows the direct measurement and mapping of many key major and minor rock-forming elements, e.g., Na, Mg, Al, Si, S, Ca, Ti, Cr, and Fe, at the surfaces of airless bodies. Remote-sensing XRF detects photons (~0.2–10 keV) emitted by atoms due to excitation by X-rays from the Sun's corona (or by energetic ions). This method has successfully been used to measure major-element surface compositions of regions of the Moon[1,2,3,4] and the asteroid 433 Eros[5,6] and more recently to globally map elemental abundances on Mercury[7,8]. Focusing optics in *CubeX*, on the other hand, enable elemental abundance measurements of planetary features with unprecedented spatial resolution and sensitivity.

Missions involving X-ray telescopes have so far been restricted to large spacecraft and telescopes with long focal lengths. For example, XMM-Newton carries three telescope modules with 7.5 m focal lengths. This was outside the realm of small satellites. Recent developments have successfully miniaturized focusing X-ray optics, enabling compact X-ray imaging spectrometers suitable for small satellites.

A second application for X-ray telescopes is the support of X-ray navigation. Deep space navigation is a critical issue for small planetary missions. XNAV can enable low-cost autonomous deep-space navigation because it can supplement or replace the oversubscribed tracking capabilities of the NASA's Deep Space Network (DSN) or ESA's European Space Tracking (ESTRACK) system. XNAV is based on timing measurements of X-ray pulsars. Again, the miniaturized X-ray optics enable those measurements on a small satellite.

In the first part of this paper we describe an X-ray telescope that can both support XRF and XNAV due to an innovative focal plane design that does not require any moving parts. The second part introduces a mission design that utilizes the unique capabilities for a lunar mission concept: Mapping the elemental composition of the regions of the Moon, which holds keys to understanding the origin and evolution of both the Moon and the Earth.

PART I: A COMPACT X-RAY IMAGING SPECTROMETER WITH PULSAR TIMING CAPABILITIES

Motivation for instrument design

The primary *CubeX* instrument is a compact X-ray imaging spectrometer (XIS) that is designed to provide insight into geology of diverse bodies in the solar system through XRF measurements. On the other hand, XRF measurements and XNAV operations share many requirements for the instrumental design. Energy range,

spatial resolution, and effective area requirements are similar, as explained in part two in the summary of the mission requirements for an example mission. The main difference is the added necessity for high resolution (<1 µs) timing measurements of pulsar pulse trains.

Even though adding that capability requires a significant change in design compared to a purely XIS instrument, the solution presented here delivers the added capabilities with minor increase in complexity.

The rationale for combining a science instrument with a navigation subsystem is an anticipated use of the instrument for deep space science investigations. For such missions, navigation cannot rely on GPS, and spacecraft navigation information is usually provided by the tracking through DSN or ESTRACK. Both can provide accurate navigation information, but they are already oversubscribed. Assuming a growing number of small satellite missions to deep space (e.g. as solicited by PSDS3 and SIMPLEx calls[9,10]), the situation will become more challenging, as more and more spacecraft are competing for limited resources. Also, as missions are moving farther away from Earth, accuracy of Earth based systems declines. XNAV could be developed into an alternative.

The following sections describe the XIS in more detail, along with an additional instrument, the Solar X-ray Monitor (SXM). The SXM monitors the solar X-ray activities in order to properly deconvolve the elemental abundance from the observed XRF, the flux and spectrum of which are dependent on the solar X-rays incidents on the lunar surface.

Instrument Overview

A spacecraft undertaking XRF measurements will carry two X-ray instruments: an X-ray Imaging Spectrometer (XIS) and a Solar X-ray Monitor (SXM) as shown in **Fig. 1**. The XIS is a small focusing X-ray telescope in a ~10 cm x 10 cm x 60 cm form factor, with a mass of just under 6 kg. It consists of Miniature Wolter-I X-ray Optics (MiXO)[11] coupled with two CMOS X-ray Active Pixel Sensors (APS) for XRF measurements[12] and a Silicon Drift Detector[13] (SDD) for XNAV observations.

The SXM is a separate SDD with a filter in a ~5 cm x 5 cm x 3 cm enclosure, designed to monitor the solar X-ray flux and its spectral evolution during XRF measurements of the lunar surface. Key instrument parameters are listed in **table 1**.

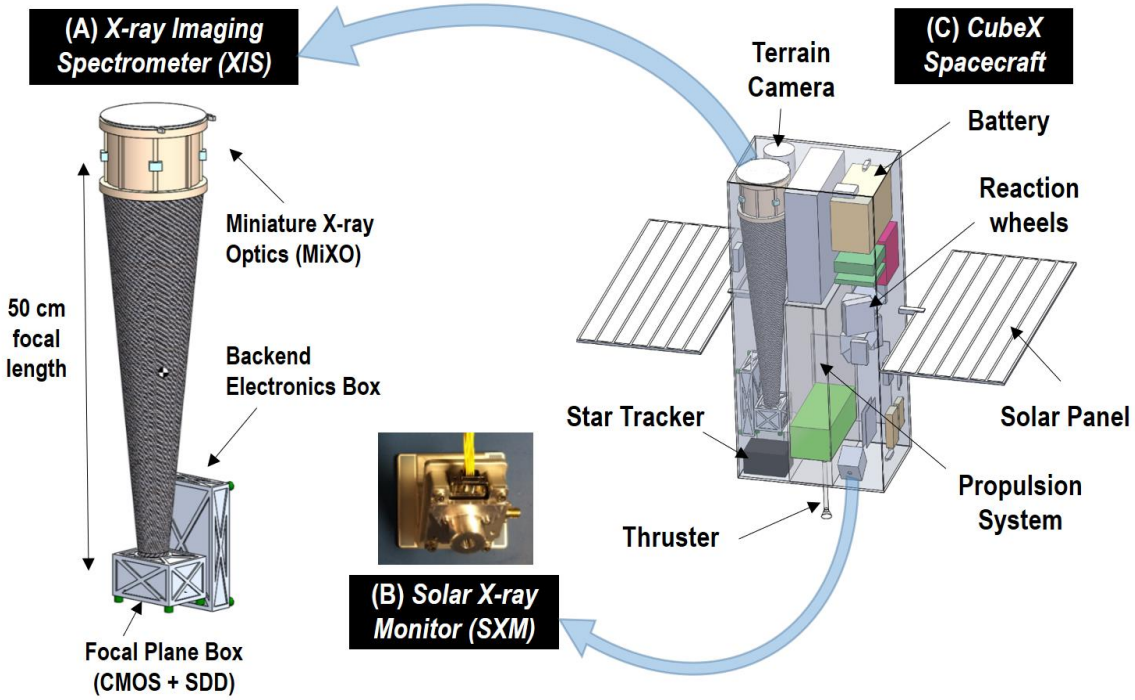

Fig. 1 Two instruments onboard *CubeX*: (A) X-ray Imaging Spectrometer (XIS) and (B) Solar X-ray Monitor (SXM) w.r.t. (C) the *CubeX* S/C. The SXM picture (not to scale) shows an actual flight model of *OSIRIS-Rex*/REXIS[14]. The SXM location is optimized for Sun viewing. Both instruments share the same electronics box. Details for focal plane and electronics are in Fig. 2.

The XIS is designed with the following features:

- High angular resolution, large collecting area and large FOV with a small focal length provided by MiXO
- High resolution imaging spectroscopy at relatively high operating temperature provided by CMOS X-ray APS
- Fast timing resolution provided by SDD.

These features are made possible, in part, by recent advances in the development of miniature X-ray optics[15,16,17] and the development of near-room temperature, radiation hard CMOS X-ray sensors.[18,19,20]

The MiXO sits on top of the XIS instrument tower. The focusing X-ray optic allows the detector area to be made much smaller than that of a non-focusing instrument, reducing the background level which scales with the size of the detector and thus improving the sensitivity by more than an order of magnitude. Located 50 cm below MiXO, the two CMOS X-ray sensors in the focal plane provide the high spectral resolution (<150 eV at 1 keV) and high spatial samplings (16 µm pixel ~6 arcsec) required to map the elemental abundances of the lunar surface through XRF imaging spectroscopy. Fast readout in the CMOS X-ray APS also enables near-room temperature operation and a wide dynamic range without pile-up, which is necessary during bright solar flares. In contrast, the spectral resolution of conventional CCDs degrades due to pile-up from the slow readout during solar flares, even though solar flares are opportune moments for XRF measurements. The SDD, a second detector mounted about 5 mm below the CMOS X-ray sensors, provides high timing resolution (< 1 µsec) necessary for precise X-ray time series measurements from millisecond pulsars (MSPs) for XNAV.

Table 1 Key XIS and SXM Parameters

Parameters	XIS	SXM
Main subsystems	MiXO + 2 CMOS for XRF + 1 SDD for XNAV	Filter +1 SDD
Volume	~10×10×60 cm	~5×5×3 cm
Mass	5.5 kg	0.3 kg
Total Power, all detectors on	8.6W (12.4W peak)	
Focal Length	50 cm	N/A
Ang. Res. FOV (footprint)	<1 arcmin (< 3 km) >1 deg^2 (>100 km)	N/A > 130 deg FWZI
Eff. Area	>20 cm^2 @ 1 keV	>2 mm^2 @ 1 keV
Energy Res. Energy Range	<150 eV @ 1 keV (CMOS) 0.6 – 4 keV (CMOS, SDD)	< 300 eV @ 6 keV 1 – 8 keV
Timing Res.	<1 µs (SDD in XIS)	4 sec (histogram)

Figure 2 illustrates the focal plane configuration with the two CMOS X-ray sensors, and the SDD. Although the FOV defined by MiXO can be covered by a single CMOS X-ray sensor, we employ two with a gap (~300 µm), and the SDD is placed behind this gap. During XRF measurements, the two CMOS X-ray sensors provide the required spectral and imaging resolution, while during XNAV operations, *CubeX* is oriented so the X-rays from MSPs fall through the gap and land on the SDD for accurate X-ray time series measurements.

This focal plane configuration is designed with no moving parts and allows these two types of detectors to receive X-rays from the same telescope. This enables both XRF measurements and XNAV operations from a single instrument.

Miniature X-ray Optic (MiXO) in XIS

Nearly all modern X-ray astronomy missions have been designed around grazing-incidence optics with Wolter-I geometries.[21] The Wolter-1 configuration combines reflections, first from a parabolic, then from a hyperbolic surface to reduce off-axis aberrations (over a single bounce system) for imaging. To increase the collecting area of these telescopes, several barrel shaped mirrors of varying diameter can be nested one inside the other along the same optical axis.

The *CubeX* X-ray optic module consists of Wolter-I X-ray mirrors, a spider alignment fixture, an outer housing, a thermal shield (TS) and a protective cover. To meet the requirements for the example mission observing the XRF of major rock forming elements (Al, Mg, Si, Ca, Fe) from the lunar surface, the design was optimized for response between 0.6 – 4 keV with full

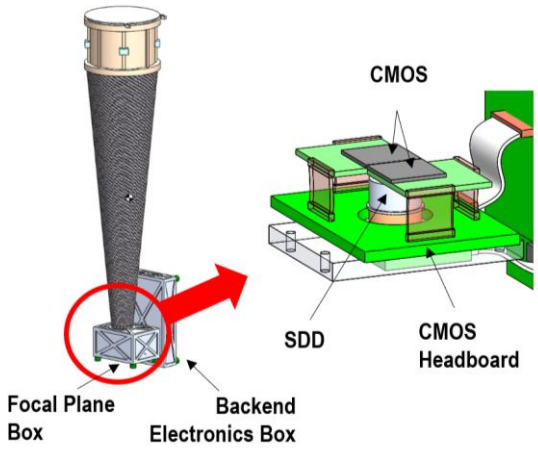

Fig. 2 XIS focal plane design: Perspective view of the two CMOS X-ray sensors and the SDD relative to backend electronics boards.

response covering 0.4 – 7 keV and angular resolution < 1 arcmin.

To cover the large footprint (~100 km at 6000 km) required by the mission, the X-ray optics FOV was set to >~60 arcmin diameter. To achieve such a large FOV within a limited SmallSat volume, the maximum diameter and length of the mirror shells was set to ~10 cm and ~8 cm, respectively. To achieve the requirement for effective area, the mirror module houses 34 nested shells, which are held in the module with an 8-spoke spider assembly on the front end.

The individual X-ray mirror shell is fabricated using the electroformed nickel replication (ENR) technique[18, 23] which has been successfully used to fabricate optics for several X-ray astronomy missions such as *Swift*/XRT, *XMM-Newton*, *Spectrum-RG*, and *FOXSI*.[24,22,25,26]

CMOS X-ray Active Pixel Sensors (APS) in XIS

The *CubeX* XRF focal plane consists of two CMOS X-ray APS optimized for X-ray, photon counting imaging spectroscopy. CMOS X-ray sensors are becoming the new state-of-the-art detector for X-ray telescopes, just as CMOS optical sensors like devices in SoloHI and WISPR are replacing CCD imagers.[22 27] For *CubeX*, we have selected the devices, known as "Big Minimal IIIs" (BM-IIIs, 1024 x 124 pixels, 16 um pixel)[18,19], which were designed by SRI/Sarnoff and share a common heritage with the flight CMOS imagers provided by SRI for other programs.

The driving requirements for the *CubeX* X-ray sensors are high spectral resolution (< 150 eV at 1 keV) to identify XRF lines from each element, large energy range (0.6 – 4 keV) to cover XRF lines from major rock forming elements such as Mg, Al, Si, and Fe (for Fe-L at 0.71 keV) and wide dynamic range to cover strong solar flares (> 3 orders of magnitude). Fast readout of the BM-IIIs enables high spectral resolution at relatively high operating temperature, and a wide dynamic range without pile-ups, which is essential during bright solar flares which can increase the X-ray flux by a few orders of magnitude. Forgiving thermal requirement (up to ~0 °C) for CMOS operation is suitable for resource-limited SmallSats. Small pixel size (~6 arcsec) is sufficient to oversample the optics PSF (~30 - 60 arcsec), and monolithic CMOS sensors have high radiation tolerance (> 100 krads) required for a long interplanetary journey and a long mission lifetime.

Silicon Drift Detector (SDD) in XIS

The XIS onboard *CubeX* will include a Silicon Drift Detector (SDD) placed behind a gap between the CMOS Active Pixel Sensors that comprise the focal plane (see **Fig. 2**). The SDD is a commercial-off-the-shelf (COTS) item designed and built by AMETEK. The SDD and its readout and control electronics are based on the design of the *NICER* instrument, successfully deployed in space on board the ISS. The *CubeX* timing accuracy requirement is more relaxed than the 100 nsec achieved by *NICER* and, thus, leaves some room to simplify the design and improve energy resolution. Note that *NICER's* timing requirement is driven by the neutron star science, not XNAV.

Solar X-ray Monitor (SXM)

The SXM is an additional instrument that monitors the solar X-ray activities to support calibration of the lunar XRF spectra received by the XIS. The solar X-ray spectrum varies by orders of magnitude in flux and spectral shape in a timeframe on the order of minutes. Therefore, simultaneous observation of the Moon and the Sun are required to properly deconvolve changes in the composition of the lunar regolith from changes in the solar X-ray spectrum.

The SXM observes the Sun using an SDD. The SXM draws significant heritage from the *OSIRIS-REx*/REXIS SXM as well as the *NICER* instrument. Both of these previous instruments also used an SDD, preamplifier, and shaping electronics to measure soft X-ray spectra with high spectral resolution. The SXM uses the detector and preamplifier from the REXIS SXM and the shaping electronics from *NICER*. In the *CubeX* SXM, the collimator is replaced with a filter to enable a wide FOV while allowing the SXM to measure the solar X-ray flux with high dynamic range.

PART II: THE *CUBEX* MISSION: LUNAR GEOLOGY AND XNAV DEMONSTRATION

Overview

This part describes the example mission with the *CubeX* instrument for lunar science.

X-ray observations of planetary bodies provide a powerful diagnostic tool for remotely determining elemental abundances including major rock forming elements such as Mg, Al, Si, and Fe since X-ray fluorescence (XRF), induced either by solar X-ray flux or energetic ions, carries decisive signatures of elemental composition. Through high-resolution XRF imaging spectroscopy, *CubeX* uses selected lunar sites to search for small patches of elusive lunar lower crust and upper mantle material excavated within and around impact craters. Informed with the surface topography from *LRO* and the gravity data from *GRAIL*, *CubeX's* measurements of regional compositional variations of lunar sites such as Schrödinger and South Pole Aitken Basins assist and provide the context for future sample return missions recommended by the Decadal Survey.

CubeX also uses high resolution X-ray imaging and time series measurements to conduct X-ray pulsar timing based navigation (XNAV) and to evaluate its performance for deep space navigation, a critical component for small planetary missions.

Mission Objectives

CubeX is a SmallSat mission that advances our understanding of the Moon's origin and evolution through measuring elemental abundances of more than 6 lunar surface regions of specific geological interest with high spatial resolution. A planetary body's bulk elemental composition is set by its formation conditions and source materials, while geological processes such as differentiation and volcanism segregate the elements into different reservoirs (e.g., primary and secondary crusts, mantle, and core). Compositional measurements are thus crucial for investigating the origin and geological evolution of the Moon and other planetary bodies. By providing such measurements, *CubeX* directly addresses the two main foci of NASA's Planetary Science Division science and research activities in Science Plan 2014, Chapter 4.3,[28] which are "*Explore and observe the objects in the solar system to understand how they formed and evolve*" and "*Advance the understanding of how the chemical and physical processes in our solar system operate, interact and evolve*."

The *CubeX* primary scientific objectives are:

(*O1*) Measure the vertical and regional composition variation of the lunar crust by determining the chemical compositions of crater central peaks, basin peak-rings, and ejecta blankets from a wide range of crater sizes (~10–200 km). e.g., Aristarchus and Finsen Craters.

(*O2*) Identify outcrops of lunar mantle on the surface (e.g., through anomalously high Mg/Si ratios), which then become possible targets for future sample return missions. e.g., Picard crater and Schrodinger Basin.

When regions of interest for the primary objectives are not observable due to viewing constraints, *CubeX* observes other regions of geological interest to address the following secondary scientific objectives:

(O3) Measure the thermal and compositional evolution of discrete lava flows of a range of ages within the same geographical regions, which provides insights into the composition and thermal evolution of the underlying mantle.[27] e.g., Regions of different ages in Oceanus Procellarum.

(O4) Measure the compositional variations of the evolved silicic volcanic feature linked to formation differences among several so-called "red spots".[30] e.g., Gruithuisen Domes.

In addition to pursuing science objectives, *CubeX* demonstrates X-ray pulsar timing-based navigation (XNAV): One of the promising approaches for autonomous deep space navigation is to use precise time series from millisecond pulsars (MSPs). Pulsars are strongly magnetized spinning neutron stars, which are the collapsed remnants of massive stars. MSPs, which spin nearly 1000 times a second, are often found isolated without a companion. Their spin rate is extremely stable, rivaling the precision of atomic clocks, due to their high mass and relatively simple structure in a compact size (~1.4 solar mass in a ~10 km diameter sphere).

The idea of using radio pulsars and X-ray pulsars as tools for S/C navigation was conceived after their discovery in the 1970s and 1980s, respectively. [31,32,33] With recent technological advances of X-ray telescopes, XNAV has become a plausible approach for realizing low-cost autonomous deep space navigation. Discoveries of MSPs have also sped up dramatically in the last decade with a set of modern X-ray and Gamma-ray telescopes such as *Fermi*. The known MSP population has doubled in the last 6 years[34] and is distributed over the whole sky, enabling 3D location and velocity determination. The two key instrumental ingredients to realize XNAV are (1) high timing resolution X-ray sensors to capture the precise X-ray time series from MSPs (~1 μsec) and (2) focusing

X-ray optics to enable efficient identification of X-rays emitted by the pulsars from the background. *CubeX* provides both and is an ideal platform to conduct XNAV and test its limits for SmallSat-size X-ray telescopes.

This translates into a technology demonstration objective for the *CubeX* mission:

(T1) Conduct X-ray pulsar based deep space navigation (XNAV) and measure its performance.

For XNAV, the plan is to observe more than 3 pulsars for >2hr per session for > 3 orbits. The prime target pulsars for XNAV operations include Crab (B0531+21), PSR B1937+21 and PSR B1821-24.[35,36]

High Level Mission requirements

High resolution imaging by the *CubeX* XIS opens a wide range of orbital configurations available for observations, which can be optimized, depending on the science goals. In comparison, with collimator instruments, the S/C often needs to stay at relatively low lunar orbits of high maintenance to achieve even minimal spatial resolution. Then, the FOV footprint, however, can only stare at a given region of the lunar surface for a very short time period each orbit (e.g., 15 deg FOV covers ~25 km on the surface for about 20 sec per orbit). Relatively short periods (~ 2 hr) of low lunar orbits (<~500 km) tend to dilute signals from a wide region of the lunar surface even during a long bright solar flare. Observations with focusing optics from high altitude orbits of a long period can collect a large portion of flare-enhanced XRF from the target region by continuously staring at the target for a few hours.

High level requirements for this mission design are:

- To observe the target regions of the Moon at C1 or higher solar states, the launch window is during next solar maximum (2023 – 2027).
- To resolve geological features of ~ 3 km scales that are likely associated with the lower crust or mantle outcrops or other features of craters, conduct observations at altitudes of < 7000 km.
- To acquire the sufficient context of the target surroundings of ~ 100 km scale, conduct observations at altitudes of > 5000 km.
- To acquire sufficient photon statistics from a target of 3 km scale at 6000 km, accumulate ~500 ksec exposure for each target.
- To improve the chance of identifying mantle and lower crust outcrops as well as the regional and vertical variation of crust composition, observe at least 6 targets including craters of various sizes including the nearside and farside of the Moon.
- To properly calibrate X-ray spectra with elemental abundance and the results of past measurements, observe at least one *Apollo* landing site for calibration.
- To measure the instrumental background, observe at least one permanently shadowed region of the Moon.

Mission Design

CubeX is designed as a secondary mission riding along a primary mission towards the moon. A quasi-frozen lunar circular polar orbit at 6000 km is selected for nominal science operations. In combination with the instrument capabilities (Tab. 1), this orbit enables successful mission completion in less than a year.

The decision to assume availability of a polar orbiting primary is based on a combination of scientific interest, past mission trends, and upcoming launch opportunities. Almost all past lunar orbiting satellites have been in polar orbits,[37] and there is scientific interest in the permanently shadowed regions of the lunar South Pole.[38,39] Hence the choice to assume deployment as a secondary from a similar orbit.

Under the assumption of a polar orbiting primary, *CubeX*'s delta-V budget is about 300 m/s, which is allocated to lunar orbit maneuvers to reach the science orbit after insertion by the primary. After the science orbit is reached, the quasi-frozen orbit requires relatively low maintenance, and will be stable enough without orbital maintenance to reach all primary science targets.

This orbit meets science requirements with no longitudinal preference in target regions of the lunar surface. The relatively lower Sun illumination of near-pole regions (i.e., the latitudinal bias of sun-illumination) is compensated to some degree by more frequent visits to near polar regions from polar orbits. The relatively long orbital period (~17 hr) enables a long (>2hr) continuous observation of each target region, which can maximize science return during long solar flares.

Spacecraft Concept

Overview

During daytime lunar science observations, the SXM views the Sun, and the XIS views the science targets. The required pointing capabilities and control authority are provided by the BCT XACT Gen3 integrated unit with flight processor, NST, sun sensor, and IMU, to which we additionally integrate reaction wheels, eight cold gas ACS thrusters, a second star tracker, sun sensors, and a standalone optical camera from Berlin Space Technologies (to provide reference position relative to the lunar surface). A gimbaled two-panel solar array provides 110W of power to a 250 Wh battery in the baseline design; omission of the gimbal is a trade to be explored in the future. Two independent propulsion systems are included: a warm gas (green) ADN fuel providing 300 m/s delta-V capability for transfer from Lunar Orbit Insertion (LOI) to the science orbit and a cold-gas system for reaction wheel momentum desaturation. The SDL PEARL integrated avionics onboard computer (OBC) is selected for command and data handling which has more than 16GB of integrated memory. A Rakon RK410 Mini USO atomic clock has been selected for XNAV and deep-space timekeeping. JPL's Iris v2.1 X-band CubeSat 32W transponder with multiple patch antennas provides communications. Finally, MLI, heaters, and temperature sensors are utilized in the thermal design.

Structures

CubeX is a small S/C, 35 cm x 23 cm x 68 cm in size, with a 13-cm rear thruster protrusion (**Fig. 8**). The 35 cm x 23 cm dimensions meet specifications for a 3U wide x 2U high canisterized satellite dispenser (CSD).

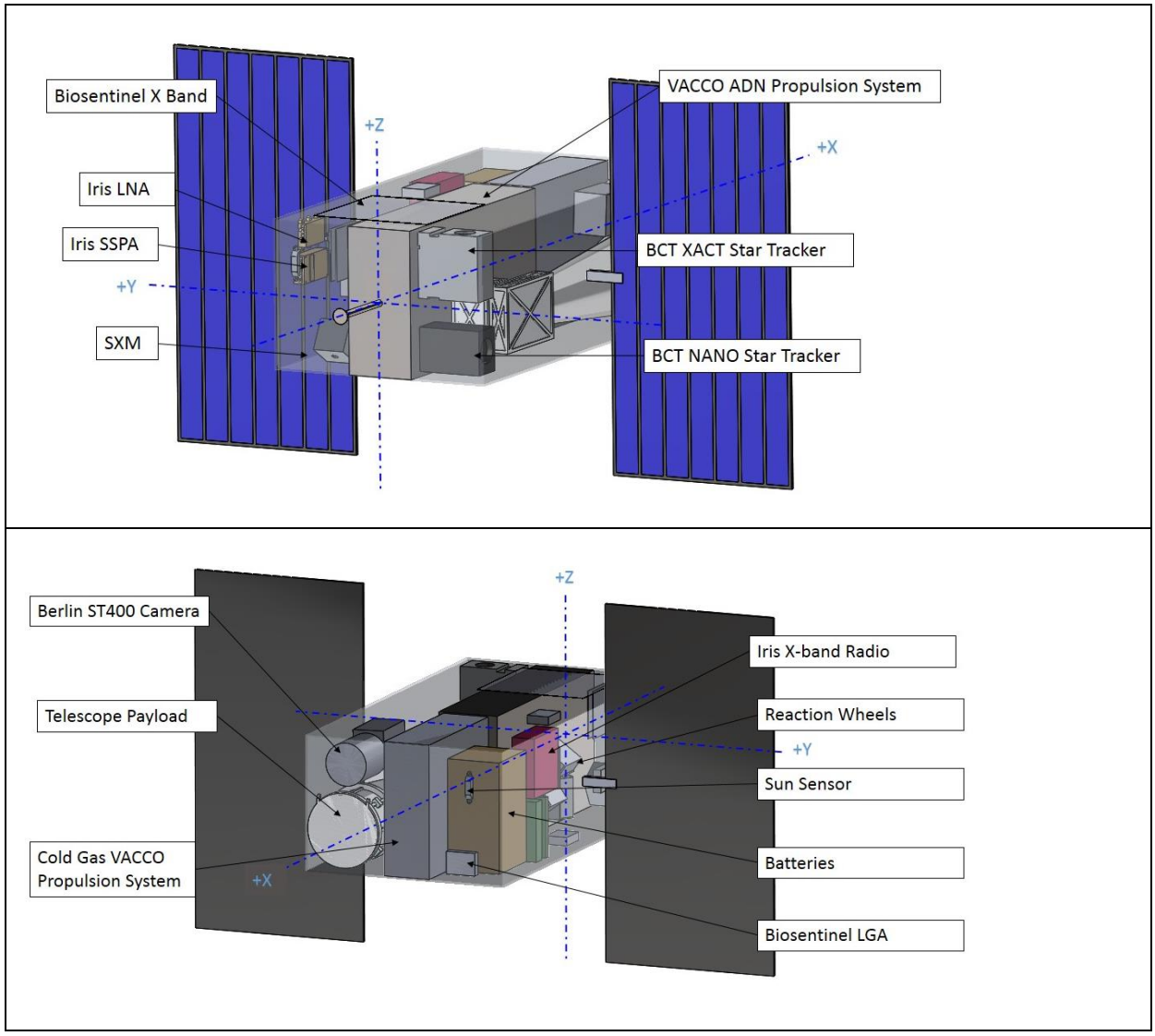

Fig. 8 *CubeX* components are packaged in a compact, SmallSat design.

The 68-cm S/C length is driven by the 60-cm XIS length plus accommodation for an optics cover mechanism and star trackers. The primary design driver for the S/C layout is the accommodation of FOVs for the instruments and various S/C components. The XIS and the Berlin ST400 camera FOVs are co-aligned to focus on the same lunar surface target for surface position verification, while the SXM has a large conical FOV and is positioned at the opposite end of the S/C to view the Sun. This layout allows the *CubeX* XIS to view lunar surface targets while the SXM has the Sun in its FoV. The radiator surface on the +Z panel, facing away from the Sun, is linked to the instrument electronics to enable thermal control.

The star trackers are mounted to the XIS focal plane to optimize pointing calibration reliability by minimizing thermal distortion. They are placed orthogonal to each other with views out the +Z and -Y panels of the structure to ensure constant orientation knowledge. The reaction wheels are co-located near the center-of-mass. The batteries, clock, X-band radio, amplifiers, and electronics card stacks are positioned to bring the center-of-mass within 2 cm of the center-of-pressure to optimize ADCS efficiency. The VACCO propulsion units, monoprop and cold gas, are symmetrical across the Y and Z planes to allow the main thruster propulsion forces to remain aligned with the center-of-mass as propellant is expended. The monoprop 5 N thruster protrudes from the center of the -X panel of the S/C. For the ADCS system, eight 10 mN cold-gas thrusters are positioned around the perimeter of the -X panel and angled such that the thruster plumes from the main thruster and ADCS thrusters do not interfere with each other.

Table 2 Propellant mass budget

Dry mass	40.3	kg
Cold-gas mass (with 30% contingency)	3.1	kg
Total dry mass to propel with VACCO green propulsion system	43.4	kg
Total mass to propel including propellant pre-estimate of 9 kg	52.4	kg
Worst-case specific impulse	239	s
CBE using worst case specific impulse	**5.9**	**kg**
Adding 10% ullage		
Adding 3% hold up		
Adding 5% propellant knowledge uncertainty		
Total mass	7.0	kg
Tank capacity	**9.0**	**kg**
Margin	**22**	**%**

Propulsion

CubeX uses an LMP-103S (ADN) non-toxic monopropellant system manufactured in partnership by VACCO Inc. and Bradford ECAPS. The VACCO ADN propulsion system consists of a single thruster developed by Bradford ECAPS that provides 5 N of nominal thrust.

The main thruster is aligned with the center-of-mass of the S/C. Liquid helium is used as a pressurant for the propellant storage. The system needs to preheat for up to 30 minutes for best performance. The advantages of the ADN propellant include 6% higher specific impulse and 24% higher density than traditional hydrazine propellant, which yields a total of 30% higher density impulse.

The *CubeX* main propulsion system is only used during the orbit acquisition phase of the mission, after the Lunar Orbit Insertion maneuver of the primary. This phase consists of a Hohmann transfer to the science orbit with an average altitude of 6000 km.

Before the maneuvers take place, the mission analysts use updated ephemeris to calculate the precise maneuver directions. Commands are upload to the S/C to specify the burn duration and align the thruster with the maneuver vector. Once the maneuvers are complete, the propulsion system remains passive unless orbit maintenance maneuvers are required for an extended mission.

For momentum management *CubeX* uses a VACCO Inc. cold gas propulsion system. Eight thrusters provide 10 mN of nominal thrust each. The propellant is R134a, which provides a specific impulse of 40-60 s. The system is based on an existing design scheduled to fly on the *MarCO* mission and will have interplanetary flight heritage before *CubeX* is launched. The cold-gas thrusters manage the main maneuvers alignment during the orbit acquisition phase and are used for desaturation maneuvers as part of the ADCS. **Tab. 2** summarizes the propellant budget.

ADCS

CubeX is a 3-axis stabilized S/C equipped with a lunar-facing terrain camera (TC), 2 star trackers, 4 reaction wheels, and an IMU consisting of a gyroscope and an accelerometer. The S/C draws from CubeSat COTS components tested for the deep-space mission, BioSentinel, and a Mars 2020 fly-by mission, *MarCO*. The *CubeX* ADCS includes the following major components:

- Three-axis gyroscope (accuracy of 1% of full-scale)
- Four sets of coarse sun sensors (±5 deg)
- Two star trackers (accuracy of 6 arcsec, 1-σ)
- Dedicated ADCS processor
- Repurposed star tracker from BST for imaging the lunar surface (resolution of 264 meters per pixel at 6000 km).

Electrical Power Subsystem

The *CubeX* power requirements were compiled from all powered components and analyzed by operational mode. The S/C requires gimbaled solar arrays capable of generating at least 110 Watts of power at end-of-life (EOL) and batteries with a minimum 250 Watt-hours of storage capacity at EOL. Additionally, the EPS must supply 12 Volts, 5 Volts, and 3.3 Volts of regulated power to the bus and perform peak power tracking operations.ctrical Power Subsystem

The solar panels are a custom MMA design based on their current HaWK series (Fig. 8.1.4-1). The design has two independently gimbaled solar panel wings with physical dimensions of ~40 cm × 60 cm. The *CubeX* batteries use the LG 18650 Li-ion cells and the SDL Pearl EPS (Fig. 8.1.4-2) for power management and distribution.

Communications

CubeX employs a single-string design for its X-band communication system. The telecommunication system provides science data downlink and telemetry, tracking and command (TT&C) via Direct-To-Earth (DTE) communication with DSN 34 m assets.

The X-band system uses JPL's Iris v2.1 transponder, Government-Furnished Equipment (GFE) for this study; a medium-gain transmit patch antenna (MGA); a low-gain (LGA) transmit antenna; and four low-gain receiving antennas (LGA).. The four receiving LGAs use a coupler that offers an approximate 180 degrees coverage per pair providing a quasi-omni receive capability to *CubeX*. Preliminary analysis shows *CubeX* can communicate with DSN 34 m at 256 kbps (max data rate for the transmitter) with link margin greater than 6 dB for both MGA and LGA.

Command and Data Handling

The C&DH uses the SDL Pearl SBC, which is currently at TRL-5 and is scheduled to be at TRL-6 in early 2018. This card has 16 GB of storage capacity, which is sufficient to store subsystem data and all mission science data, giving ultimate flexibility to transmit the data whenever suitable.

Thermal

The following is a description of the approach taken to meet the thermal requirements of *CubeX*. To maintain the XIS optics at +20 °C, the optics assembly is isolated from the S/C structure. A thermal shield (TS) on the optics assembly minimizes radiative heat loss to space. The shield is a thin plastic film coated by aluminum which has a low solar absorptance and a low infrared emissivity. A heater is mounted on the optics assembly housing to control and maintain its temperature at 20 °C.

The SDD assembly unit and the CMOS detectors of the XIS instrument are temperature controlled at –20 °C. These XIS components as well as the SXM are thermally anchored to a radiator that is mounted on the outside of the S/C. The radiator location is chosen such that its temperature is sufficiently low at all times during the science operations to ensure the –20 °C temperature control of XIS can be achieved. A Thermal Electric Cooler (TEC) is employed to cool XIS' SDD detector to below –50 °C. The temperature of the SXM's SDD detector is also maintained below –50 °C by employing a second TEC. The XIS backend electronics box which contains the CMOS and SDD boards is temperature controlled at ~+30 °C. The temperature of the battery pack is controlled as well using a trim heater.

Several representative orbits that impose the most extreme thermal conditions on *CubeX* are analyzed using Thermal Desktop. The current design meets the requirements, but further analysis will be required when the design solidifies.

SUMMARY AND OUTLOOK

With the advances in X-ray optics, XRF measurements are now feasible with a compact instrument. For deep space applications, the *CubeX* focal plane design combines XRF spectroscopy capabilities with X-ray timing measurements that enable XNAV from the same payload. The presented lunar mission provides insight into the lunar geology. However, while the fundamental quest for understanding the origin and evolution of the Moon motivates the *CubeX* concept and design, XIS' small form factor (~1×1×6 U), mass (<6 kg), and power consumption (<9 W) open the door to a wide range of applications for various targets and missions including NEOs and Martian moons. A large number of low-cost *CubeX* S/C could revolutionize our understanding of NEOs and other airless bodies through rapid deployment to multiple targets.

ACKNOWLEDGEMENTS

This work was sponsored, in part, under NASA award No. NNX17AK29G in support of the Planetary Science Deep Space Smallsat Studies, NASA Solicitation NNH16ZDA001N-PSDS3. The authors would like to thank the management of NASA Ames Research Center for their support, especially Jay Bookbinder.

REFERENCES

1. Adler, I., Trombka, J., Gerard, J., Lowman, P., Schmadebeck, R., Blodget, H., … & Bjorkholm, P. (1972). Apollo 15 Geochemical X-ray Fluorescence Experiment: Preliminary Report. Science, 175(1), 436-440.
2. Adler, I., Trombka, J., Gerard, J., Lowman, P., Schmadebeck, R., Blodget, H., … & Harris, B. (1972). Apollo 16 Geochemical X-ray Fluorescence Experiment: Preliminary Report. Science, 177(7), 256-259. doi:10.1126/science.177.4045.256
3. Narendranath, S., Athiray, P. S., Sreekumar, P., Kellett, B. J., Alha, L., Howe, C. J., ... & Unnikrishnan, U. (2011). Lunar X-ray fluorescence observations by the Chandrayaan-1 X-ray Spectrometer (C1XS): Results from the nearside southern highlands. Icarus, 214(1), 53-66.
4. Weider, S. Z., Kellett, B. J., Swinyard, B. M., Crawford, I. A., Joy, K. H., Grande, M., ... & Anand, M. (2012). The Chandrayaan-1 X-ray spectrometer: First results. Planetary and Space Science, 60(1), 217-228.
5. Trombka, J. I., Squyres, S. W., Brückner, J., Boynton, W. V., Reedy, R. C., McCoy, T. J., ... & Nittler, L. R. (2000). The elemental composition of asteroid 433 Eros: Results of the NEAR-Shoemaker X-ray spectrometer. Science, 289(5487), 2101-2105.
6. Nittler, L. R., Starr, R. D., Lev, L., Mccoy, T. J., Burbine, T. H., Reedy, R. C., ... & Mcclanahan, T. P. (2001). X-ray fluorescence measurements of the surface elemental composition of asteroid 433 Eros. Meteoritics & Planetary Science, 36(12), 1673-1695.
7. Nittler, L. R., Starr, R. D., Weider, S. Z., McCoy, T. J., Boynton, W. V., Ebel, D. S., ... & Lawrence, D. J. (2011). The major-element composition of Mercury's surface from MESSENGER X-ray spectrometry. Science, 333(6051), 1847-1850.
8. Weider, S. Z., Nittler, L. R., Starr, R. D., Crapster-Pregont, E. J., Peplowski, P. N., Denevi, B. W., ... & Solomon, S. C. (2015). Evidence for geochemical terranes on Mercury: Global mapping of major elements with MESSENGER's X-Ray Spectrometer. Earth and Planetary Science Letters, 416, 109-120.
9. Planetary Science Deep Space Smallsat Studies, NASA Solicitation NNH16ZDA001N-PSDS3 (2016),https://nspires.nasaprs.com/external/solicitations/summary.do?method=init&solId=%7BDF68AD7A-2E90-746B-21A4-C6528A7C6B4F%7D&path=init
10. Small Innovative Missions for Planetary Exploration (SIMPLEx), NASA Solicitation NNH17ZDA004O-SIMPLEX (2018), https://nspires.nasaprs.com/external/solicitations/summary!init.do?solId={523A5AF4-07C1-1FA4-0734-9C0253A172DF}&path=open
11. Hong, J., & Romaine, S. (2016). Miniature lightweight X-ray optics (MiXO) for surface elemental composition mapping of asteroids and comets. Earth, Planets and Space, 68(1), 35.
12. Kenter, A. T., Kraft, R., & Murray, S. S. (2012, September). Development of monolithic CMOS detectors as x-ray imaging spectrometers. In Proc. of SPIE Vol (Vol. 8453, pp. 84530G-1).
13. Gendreau et al. (2016) "The Neutron star Interior Composition Explorer (NICER): design and development", Proceedings of the SPIE, Volume 9905, id. 99051H 16 pp.
14. Masterson et al. (2018) "Regolith X-Ray Imaging Spectrometer (REXIS) Aboard the OSIRIS-REx

Asteroid Sample Return Mission", Space Science Reviews, Volume 214, 26 pp.

15. N15 Romaine S., Bruni R., Choi B., Gorenstein P., Jensen C., Ramsey B., Rosati R., Sampath S. (2013). Development of light weight replicated x-ray optics. In SPIE Optical Engineering Applications (Vol. 8861). San Diego, CA. doi:10.1117/12.2024897

16. N16 Romaine, S., Bruni, R., Choi, B., Jensen, C., Kilaru, K., Ramsey, B., & Sampath, S. (2014, July). Development of light weight replicated x-ray optics, II. In Space Telescopes and Instrumentation 2014: Ultraviolet to Gamma Ray (Vol. 9144, p. 91441H). International Society for Optics and Photonics.

17. N17 Hong, J., Romaine, S., Ramsey, B., Nittler, L., & Grindlay, J. (2016). Developing Miniature Wolter-I X-Ray Optics for Planetary Science. LPI Contributions, 1980.

18. Janesick, J., Pinter, J., Potter, R., Elliott, T., Andrews, J., Tower, J., Cheng, J., & Bishop, J.(2009, August). Fundamental performance differences between CMOS and CCD imagers: part III. In Society of Photo-Optical Instrumentation Engineers (SPIE) Conference Series, 7439.

19. Janesick, J., Pinter, J., Potter, R., Elliott, T., Andrews, J., Tower, J., Grygon, M., & Keller, D.(2010, July). Fundamental performance differences between CMOS and CCD imagers: part IV. In Society of Photo-Optical Instrumentation Engineers (SPIE) Conference Series, 7742.

20. Kenter, A. T., Kraft, R., & Murray, S. S. (2012, September). Development of monolithic CMOS detectors as x-ray imaging spectrometers. In Proc. of SPIE Vol (Vol. 8453, pp. 84530G-1).

21. Wolter, H. (1975). Mirror systems with grazing incidence as image-forming optics for x-rays. Mirror systems with grazing incidence as image-forming optics for X-rays Transl. into ENGLISH from Ann. Phys.(Leipzig), ser. 6, v. 10, 1952 p 94-114.

22. N22 Jansen, F., Lumb, D., Altieri, B., Clavel, J., Ehle, M., Erd, C., ... & Munoz, R. (2001). XMM-Newton observatory-I. The spacecraft and operations. Astronomy & Astrophysics, 365(1), L1-L6.

23. Citterio, O., Conconi, P., Ghigo, M., Mazzoleni, F., Pareschi, G., & Peverini, L. (2000, November). Development of soft and hard X-ray optics for astronomy. In X-Ray Optics, Instruments, and Missions IV (Vol. 4138, pp. 43-57). International Society for Optics and Photonics.

24. Burrows, D. N., Hill, J. E., Nousek, J. A., Wells, A. A., Short, A. D., Willingale, R., ... & Campana, S. (2000, July). The swift x-ray telescope. In Proc. SPIE (Vol. 4140, pp. 64-75).

25. Pavlinsky, M., Sunyaev, R., Churazov, E., Gilfanov, M., Vikhlinin, A., Hasinger, G., ... & Ohashi, T. (2008, July). Spectrum-roentgen-gamma astrophysical mission. In Proc. of SPIE Vol (Vol. 7011, pp. 70110H-1).

26. Krucker, S., Christe, S., Glesener, L., Ishikawa, S. N., McBride, S., Glaser, D., ... & Saito, S. (2011). The Focusing Optics x-ray Solar Imager: FOXSI. NASA Goddard Space Flight Center; Greenbelt, MD.

27. Korendyke, C. M., Vourlidas, A., Plunkett, S. P., Howard, R. A., Wang, D., Marshall, C. J., ... & Tower, J. (2013, October). Development and test of an active pixel sensor detector for heliospheric imager on solar orbiter and solar probe plus. In SPIE Optical Engineering+ Applications (pp. 88620J-88620J). International Society for Optics and Photonics.

28. United States of America, National Aeronautics and Space Administration, Science Mission Directorate. (2014). Science Plan (pp. 60-73). Washington, DC: NASA Headquarters. Retrieved from https://science.nasa.gov/about-us/science-strategy.

29. Crawford, I. A., Joy, K. H., Kellett, B. J., Grande, M., Anand, M., Bhandari, N., ... & Goswami, J. (2009). The scientific rationale for the C1XS X-ray spectrometer on India's Chandrayaan-1 mission to the moon. Planetary and Space Science, 57(7), 725-734.

30. Glotch, T. D., Lucey, P. G., Bandfield, J. L., Greenhagen, B. T., Thomas, I. R., Elphic, R. C., ... & Paige, D. A. (2010). Highly silicic compositions on the Moon. *science*, *329*(5998), 1510-1513.

31. Reichley, P., Downs, G., & Morris, G. (1971). Use of pulsar signals as clocks. JPL Quart. Tech. Rev, 1(2), 80-86.

32. Downs, G. S. (1974). Technical Report 32-1594 Interplanetary Navigation Using Pulsating Radio Sources (pp. 1-19) (United States of America, National Aeronautics and Space Administration). Pasadena, CA: Jet Propulsion Laboratory.

33. Chester, T. J., & Butman, S. A. (1981). Navigation using X-ray pulsars. Jet Propulsion

Laboratory, Pasadena, CA, NASA Tech. Rep. 81N27129.

34. Özel, F., & Freire, P. (2016). Masses, radii, and the equation of state of neutron stars. Annual Review of Astronomy and Astrophysics, 54, 401-440.

35. Shemar, S., Fraser, G., Heil, L., Hindley, D., Martindale, A., Molyneux, P., ... & Lamb, A. (2016). Towards practical autonomous deep-space navigation using X-Ray pulsar timing. Experimental Astronomy, 42(2), 101-138

36. Winternitz, L. M., Mitchell, J. W., Hassouneh, M. A., Valdez, J. E., Price, S. R., Semper, S. R., ... & Gendreau, K. C. (2016, March). SEXTANT X-ray Pulsar Navigation demonstration: Flight system and test results. In Aerospace Conference, 2016 IEEE (pp. 1-11). IEEE.

37. Plice, L., & Craychee, T. (2011). A Design Method for Low Altitude, Near-Equatorial Lunar Orbits. Advances in the Astronautical Sciences, 142.

38. Mitrofanov, I. G., Sanin, A. B., Boynton, W. V., Chin, G., Garvin, J. B., Golovin, D., ... & Malakhov, A. (2010). Hydrogen mapping of the lunar south pole using the LRO neutron detector experiment LEND. Science, 330(6003), 483-486.

39. Schultz, P. H., Hermalyn, B., Colaprete, A., Ennico, K., Shirley, M., & Marshall, W. S. (2010). The LCROSS cratering experiment. Science, 330(6003), 468-472.